A NEW POWER MEMS COMPONENT WITH VARIABLE CAPACITANCE

T. Sterken[1,2], K. Baert[1], R. Puers[2], G. Borghs[1,2], R. Mertens[1,2]
[1]IMEC vzw, Kapeldreef 75, 3001 Leuven, Belgium
[2]ESAT, K.U.Leuven, Kasteelpark Arenberg 10, 3001 Leuven, Belgium
Tom.Sterken@imec.be

ABSTRACT
Autonomous devices such as wireless sensors and sensor networks need a long battery lifetime in a small volume. Incorporating micro-power-generators based on ambient energy increases the lifetime of these systems while reducing the volume. This paper describes a new approach to the conversion of mechanical energy, available in vibrations, to electrical energy. The conversion principle is based on charge transportation between two parallel capacitors. An electret is used to polarize the device. A large-signal model was developed, allowing simulations of the behavior of the generator. A small-signal model was then derived in order to quantify the output power as a function of the design parameters. These models show the possibility of generating up to 40 μW with a device of 10 mm^2. A layout was made based on a standard SOI-technology, available in an MPW. With this design a power of 1 μW at 1020 Hz is expected.

Keywords: micro-generator, electret, modeling, SOI

INTRODUCTION
Continuous miniaturization of electronics together with large-scale integration leads to the development of very small, but complex systems on a chip (SOC) or in a package (SOP). The small volume and weight of the systems enables mobile use, for which communication is a very important issue. Ad hoc wireless networks are based on these systems, leading towards Ambient Intelligence. They are necessary to sense and properly process information for medical applications or to enhance human comfort. Other applications that benefit from wireless networks are sensors positioned on places that are difficult to contact. They consist of small autonomous nodes, which are able to sense, process data, communicate and control the data traffic, while consuming extremely low power to ensure a high lifetime.
Due to progress in technology, combined with low-power design, the power consumption of a microprocessor has gone below 1 μW [1]. The power needed for transmission strongly depends on the environmental conditions and performance issues such as signal to noise ratio, carrier frequency and transmission distance. A biomedical communication channel over 35 cm consumes about 3 mW [2,3].
The average power dissipation of one node then strongly depends on the transmission duty cycle (typically about 0.33%) [4] and varies between 0.065 and 22.5 mW [3,5].

Currently, autonomous systems are powered by electrochemical batteries. Although the energy density of primary batteries is about three times higher than the density of rechargeable batteries, the lifetime they can guarantee (with a given volume limited by the device specifications) is often not sufficient, due to self discharge and the volume occupied by the package [6]. This problem can be solved by using energy carriers with higher energy densities and/or by using rechargeable batteries.
The first solution consists of energy carriers such as nuclear material (1.5 GJ/cm^3) or combustion fuels (35 kJ/cm^3) [7]. The practical use of nuclear materials is limited to space applications, as the uncontrolled spread of nuclear sources in small power sources is intolerable for terrestrial applications. Although the design of micro-combustion engines is troubled by thermal management and multiwafer processing, work in this field has been done by MIT [8]. A micro-turbine suited for use with micro-combustors was developed by K.U.Leuven [9].
A highly efficient way to convert the energy stored in combustion fuels is a fuel cell, which converts the energy electro-chemically. Research on methanol (17 kJ/cm^3) fuel cells at Carnegie Mellon University suggests a power of 10 mW for a 15 cc device, running for 5 weeks [10].
Even the lifetime of a high-density energy storage device is limited by the available volume. A solution to this problem is the use of rechargeable storage devices, such as secondary batteries, supercapacitors, rechargeable fuel cells or rechargeable combustors. This solution is only adequate in case the recharging process does not require a big effort (e.g. GSM, laptop). Storage systems that are incorporated into solid structures or implanted in vivo, can also be recharged, e.g. through RF-links [11].

If the number of autonomous nodes increases another problem arises: as the network nodes are distributed over a large area, the recharging is not efficient and in some cases (e.g. smart dust and incorporated or implanted nodes) not feasible. Those systems would benefit from *in situ* power generators. Depending on the specifications of this generator the volume of the battery decreases and the theoretical lifetime becomes infinite.
These microgenerators convert energy available in the ambient to electrical energy. The energy source depends on the application. Typical energy-sources are light (photovoltaic energy), heat (thermal energy), vibrations (mechanical energy), flow (wind, fluidics) or bio-fuel (glucose). In case more than one form of energy is available the autonomous system may benefit from a combined system, where the temporary lack of one source is complemented by another energy-form (e.g. photovoltaic energy during day-time and mechanical energy during the night).

In this paper we consider electromechanical converters realized by MEMS processing. These converters are based on one of the following three principles: electromagnetic, electrostatic or piezoelectric transduction. In electromagnetic transducers a magnet is attached to a seismic mass on a spring. This makes the system sensitive to vibrations from the housing. The magnetic field of the magnet is coupled to an inductor which is

fixed to the housing. The varying magnetic field induces an m.m.f. on the inductor, which delivers power to an electrical load. As this coupling is basically a three-dimensional phenomenon miniaturization is limited and planar Si processing is not straightforward. Nevertheless *Li et al.* realized a prototype which could deliver 680 μW at 60-110 Hz for an input vibration of 200 μm [12].

A piezo-electric converter was proposed by *Glynne-Jones et al.* [13]. Again a seismic mass is attached to a spring. As the spring is bended, a piezo-electric material is deformed, inducing charges on two electrodes. The resulting charge transport delivers energy to an external circuit. A good generator is feasible, as concluded by Glynne-Jones, if material properties can be achieved comparable to bulk PZT.

An electrostatic energy-converter consists of a variable capacitor, of which the capacitance is sensitive to external vibrations. Previous attempts where realized by MIT [14] and Berkeley [15], using an electronic control circuit to charge a variable capacitor. The energy of this charge is increased mechanically, resulting in a net energy gain when the capacitor is discharged.

Another principle of electrostatic energy conversion is used in this paper: a variable capacitor is polarized by an *electret*, i.e. a fixed charge distribution in a dielectric material, inducing an equivalent voltage over the variable capacitor. Due to an external vibration the capacitances of the polarized variable capacitors will change, varying the charge on the plates according to $Q = CV$. This charge transport delivers power to the load circuit. Polarization by electrets has successfully been used in electrostatic microphones and MEMS-based electret microphones [16,17].

DEVICE

A schematic cross-section of the device is given in Fig. 1. It consists of a standard lateral comb resonator which is suspended by clamped beams, acting as springs between the mass and the substrate. External vibrations induce a relative displacement of the mass in the indicated direction. As the overlap of the fingers varies, the capacitance changes. The variable capacitors are polarized by means of an electret, which is a fixed charge distribution in a dielectric layer.

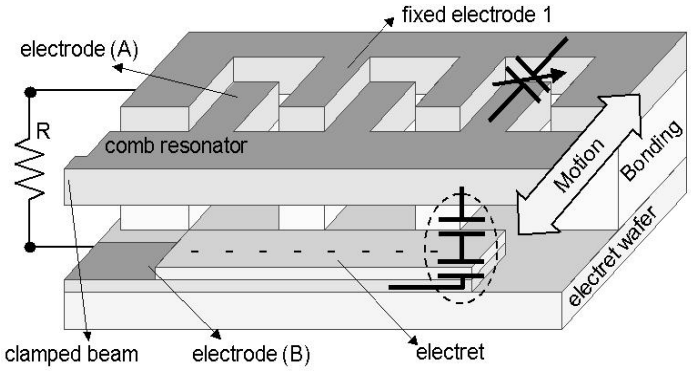

Figure 1: Cross-section through the device. The other side of the device (fixed electrode 2) is symmetric to the one shown.

The electret induces an electric field between the plates, as indicated in Fig. 2.

The device has four electrodes: two fixed electrodes, a movable electrode (*electrode A*) and the electret contact (*electrode B*).

The resistors connected between the fixed electrodes and electrode B represent the load circuit, including power conditioning electronics and if necessary a storage system such as micro-batteries.

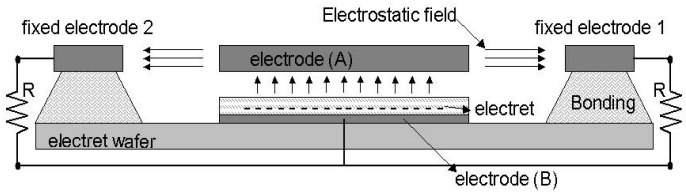

Figure 2: Side-view of the structure, illustrating the electrostatic field in the system, and the

Principle

The equivalent electrical circuit of the device is given in Fig. 3, indicating the variable capacitors C_1 and C_2, the load resistors R and the electret carrying the fixed charge Q.

A charge Q is induced by the electret on electrode A, and is proportionally distributed between C_1 and C_2 into a charge Q_1 on C_1 and a charge Q_2 on C_2 as indicated by (1):

$$Q_1 = \frac{C_1}{C_1 + C_2} Q \qquad Q_2 = \frac{C_2}{C_1 + C_2} Q \tag{1}$$

The variable capacitors change complementary: by changing the capacitance C_1 to $C_1+\Delta C$, C_2 changes to $C_2-\Delta C$. The charge Q_1 increases by the same amount ΔQ as the charge Q_2 decreases:

$$\Delta Q = \frac{\Delta C}{C_1 + C_2} Q \tag{2}$$

The charge transport gives rise to a current, which supplies energy to the external circuit. This energy originates from the mechanical vibrations responsible for the capacitance change.

Note that the current between electrodes A and B is zero, due to the symmetric structure. The resistance of this branch does not introduce any unwanted losses, which facilitates the design of the movable electrode.

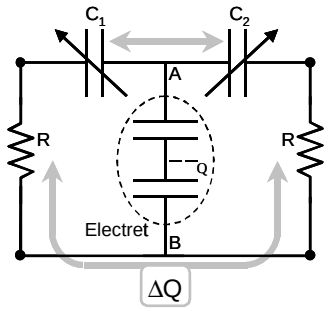

Figure 3: Principle scheme of the electret based generator.

MODELING

To obtain a good insight into the working principles of the device and to quantify the power generation, a qualitative model is needed. The equivalent electrical circuit of Fig. 3 does not fulfill these requirements, as the correlation between the mechanical vibration of the device and the variation of the capacitances is not included. The electret and the comb resonator are modeled separately and combined afterwards. We will illustrate the feasibility of generating power with an electret-based generator by modeling a device with typical dimensions. This illustrative device will nevertheless not be realized in this paper: to obtain feedback on the modeling a demonstrator has been designed in a commercially available technology. As a result this demonstrator is not optimized towards a maximum power.

Electret

The fixed charge layer is modeled in Fig. 3 by a charged node between two capacitors. This intuitive representation is correct for homopolar electrets, which mainly consist of an excess of charges with one polarity. A second type of electrets consists of mainly neutral dielectrics, which are polarized (heteropolar electrets). The charges are fixed by charge traps, mostly at the surfaces. If two dielectrics are used, charge traps also appear at the interface between the two materials [18].

Consider a dielectric (with dielectric constant ε_r) clamped between two electrodes (Fig. 4a), which has a charge layer (with density σ) fixed at a distance d from one of the electrodes. By applying Gauss' law the following relationship is found between the applied voltage V on the electrodes and the charge q on the top electrode:

$$V = q\frac{1}{C_{tot}} + \sigma\frac{d}{\varepsilon_0\varepsilon_r} = q\frac{1}{C_{tot}} + V_{elec} \qquad (3)$$

The permittivity of the vacuum is given by ε_0, while C_{tot} represents the capacitance between the two electrodes, if no charges where trapped. The same method applied to heteropolar electrets generates the same formula (3), where d now indicates the distance between the two charge-layers (Fig. 4b).

Any electret is thus modeled by the series of a voltage source V_{elec} and a capacitor C_{tot}. Typical values for the charge density go up to 0.5 μC/cm^2 for 1 μm thick SiO_2, corresponding to an electret voltage of -145 V [19].

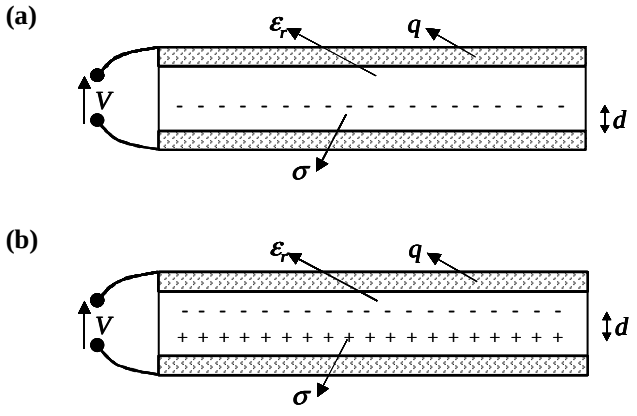

Figure 4: (a) Homopolar and (b) heteropolar electrets.

Illustrative device

To illustrate the feasibility of the generation method we will consider a comb structure with a thickness of 100 μm, a length of 5 mm and a mass width of 1 mm. The fingers are etched by high aspect ratio RIE and have a width of 5 μm. The gap is also 5 μm, so each side has 250 fingers and 500 capacitors. These fingers have a length of 250 μm, with an initial overlap of 100 μm. Due to 1 μm underetch, the effective gap spacing will be about 6 μm. The total surface occupied is about 0.1 cm^2, while the electret surface is only 0.05 cm^2. The gap between the electret surface and the variable capacitor is 1 μm.

Variable capacitor

A correct model for the variable capacitor has to link both mechanical and electrical sides. The modeling is done for a single variable capacitor instead of for the two complementary capacitors, to ease the calculations. This model is build based on the energy function of the capacitor [20]:

$$E = \frac{\delta}{2N\varepsilon_0 d}\frac{Q_1^2}{(h-x)} \qquad (4)$$

where E is the energy in the stored in the two capacitors, and the symbols are according to:

Symbol		Common Values
Q_1	charge on the capacitor	920 pF
δ	gap spacing	6 μm
N	number of capacitors	500
b	thickness of the fingers	100 μm
h	initial overlap of the fingers	100 μm
x	displacement of the mass	

The derivatives of this energy function to the displacement and the charge result in relationships between the mechanical force and the electrical voltage, and the displacement and the charge. These non-linear equations are given by:

$$\begin{cases} F_e = \frac{1}{2}\frac{Q_1^2\delta}{N\varepsilon_0 b(h-x)^2} \\ V = \frac{Q_1\delta}{N\varepsilon_0 b(h-x)} \end{cases} \qquad (5)$$

This large-signal model was implemented in SPICE, using Verilog-A–language, to simulate the energy-conversion of the device as response to an external vibration. This language allows the user to define an instance with the required behavior. Fig. 5 illustrates how a single-sided capacitor is implemented in SPICE.

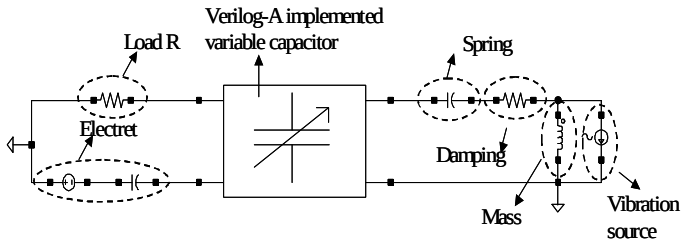

Figure 5: Large-signal model implemented in SPICE. The square two-port models the variable capacitor according to equations (5).

The two-port represents the Verilog-A instance. The mechanical lumped elements (mass, spring and damping) are implemented as their equivalent electrical components (respectively inductor, capacitor and resistor) [21].
This non-linear model does not allow the extraction of an analytical relation between the input parameters and the output power as function of the design parameters.
Therefore equations (5) were linearized to *x* and *Q* to study the behavior of a varying overlap capacitor, which will be called C_0 to stress that the analysis is based on single capacitor instead of two complementary capacitors. The resulting linear equations are linked to a lumped element equivalent electrical circuit [21].

The combination of the capacitor model, the electret model and the equivalent circuit for the mechanical parts of the device leads to the lumped-element circuit of Fig.6.
The vibration is modeled as a sinusoidal current source. In this model C_{elec} is the total capacitance between the movable electrode and electrode (B). These electrodes are shaped in such a way that the capacitance C_{elec} is constant for any displacement of the movable electrode. The equivalent electret voltage is divided between this capacitor C_{elec} and the variable capacitor. The capacitance C_{elec} has to be much larger than C_0 to obtain a good polarization.

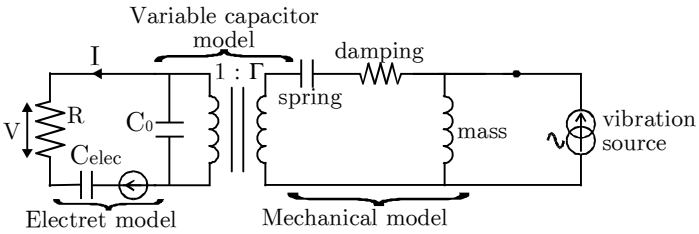

Figure 6: Lumped element model of 1 variable capacitor.

The parameters in Fig. 6 are:

Symbol		Typical Values
Γ	transformation factor	9.28 µC/m
C_0	static capacitance of one side	7.4 pF
Y	vibration amplitude	5 µm
C_{elec}	capacitance between electrode (B) and comb structure	44 pF

Parameter Γ represents the transformation factor (in C/m or N/V). It is given by the charge on the capacitor at rest (928 pC) divided by the initial overlap *h*.
The power output of this circuit as a function of the design parameters, the input vibration amplitude and frequency is given by standard circuit analysis:

$$P(\omega)=\frac{\left(\frac{\omega}{\omega_1^*}\right)^4\left(\frac{\omega}{\omega_2}\right)^2\frac{\Gamma^2}{C_0^2}\frac{Y^2}{2R}}{\left(\alpha-\left(\frac{\omega}{\omega_1^*}\right)^2-2\zeta^*\frac{\omega^2}{\omega_2\omega_1^*}\right)^2+\left(\frac{\omega}{\omega_2}\right)^2\left(1-\left(\frac{\omega}{\omega_1^*}\right)^2+2\zeta^*\frac{\omega_2}{\omega_1^*}\right)^2} \quad (6)$$

In this formula ω_1 refers to the mechanical resonance frequency, while ω_2 represents the cut-off frequency of the electrical filter formed by the load, the combination of the variable capacitor and the electret capacitance:

$$\omega_1=\sqrt{\frac{k}{m}} \qquad \omega_2=\frac{C_0+C_{elec}}{RC_0C_{elec}} \quad (7)$$

All parameters indicated with a * are influenced by the electromechanical interaction, their value depends on the coupling factor κ between the mechanical and the electrical domain:

$$\kappa^2=\frac{1}{1+\frac{C_0k}{\Gamma^2}} \qquad \omega_1^*=\frac{\omega_1}{\sqrt{1-\kappa^2}}=\sqrt{\frac{k+\frac{\Gamma^2}{C_0}}{m}} \quad (8)$$

In these equations k and m are respectively the spring constant (30 N/m) and the mass (1.2 mg). The mechanical resonance frequency ω_1 is then 4995 rad/s (or 795 Hz), while ω_1^* is shifted to 5820 rad/s (or 926 Hz).
The coupling factor κ, which represents the ratio between the converted energy and the stored energy, is 50,8 %.
The damping *d*, due to the viscosity of air, is about 100 Ns/m and is related to the damping coefficient by:

$$\zeta=\frac{d}{2m\omega_1} \quad (9)$$

while

$$\zeta^*=\frac{d}{2m\omega_1}\sqrt{1-\kappa^2}=\frac{d}{2m\omega_1^*} \quad (10)$$

The output power is plotted in Fig.7 as a function of the frequency, for the following three different loads (3 MΩ, 10 MΩ and 100 MΩ). These loads lead to the following cut-off frequencies:

Load	Cut-off frequency
3 MΩ	8370 Hz
10 MΩ	2512 Hz
100 MΩ	251 Hz

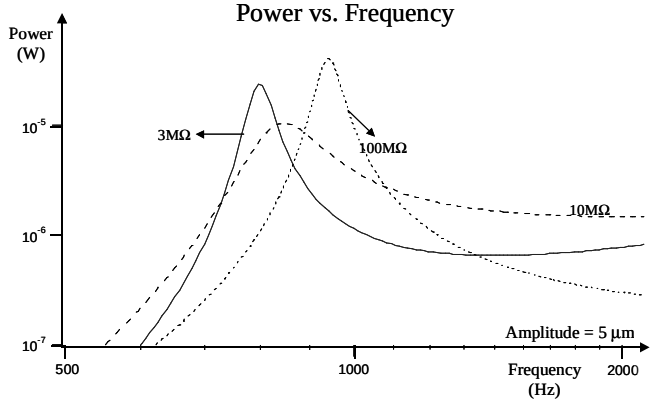

Figure 7: Power curves for the illustrator device as a function of the frequency. The resonance shifts due to load matching.

The maximum power of 40 µW is reached at 930 Hz (for 100 MΩ). This is equivalent to 400 µW /cm^2.

Modeling discussion
The basic behavior of the system (equation (6)) is more interpretable if mechanical damping is neglected:

$$P_{damping=0}(\omega)=\frac{\left(\frac{\omega}{\omega_1^*}\right)^4\left(\frac{\omega}{\omega_2}\right)^2\frac{\Gamma^2}{C_0^2}\frac{Y^2}{2R}}{\left(\alpha-\left(\frac{\omega}{\omega_1^*}\right)^2\right)^2+\left(\frac{\omega}{\omega_2}\right)^2\left(1-\left(\frac{\omega}{\omega_1^*}\right)^2\right)^2} \quad (8)$$

This equation is dominated by the cut-off frequency ω_2 of the filter formed by the load and the two parallel capacitors: C_0 and C_{elec}. If the load is very high, as for accelerometers, this cut-off frequency is very low, and the power is determined by the second term in the denominator. The system resonates at frequency ω_1^*. This resonance frequency is always higher than the mechanical resonance frequency ω_1.

In the other case (low load resistance), the cut-off frequency is much higher than the working frequencies (which are around the resonance frequency). In this case the resonance frequency is determined by the factor α :

$$\alpha=\frac{C_0+(1-\kappa^2)C_{elec}}{C_0+C_{elec}} \quad (11)$$

$$\omega_{res}=\alpha\omega_1^*=\sqrt{\frac{k+\Gamma^2/(C_0+C_{elec})}{m}} \quad (12)$$

As the electret capacitance has to be higher than C_0 to obtain a good polarization, this resonance frequency practically equals ω_1. The shift of the resonance frequency allows the load circuit to change the generators behavior by changing the applied load.

For each working frequency there exists an optimal load resistance for which the power at that frequency is optimized, determined by equation (13). This results in a maximum power given by equation (14).

$$\omega_2(\omega)=\omega\frac{1-\left(\omega/\omega_1^*\right)^2}{\alpha-\left(\omega/\omega_1^*\right)^2} \quad (13)$$

$$P_{\max,\zeta=0}(\omega)=\frac{\frac{\Gamma^2}{C_0^2}\frac{Y^2}{4}\frac{C_0C_{elec}}{C_0+C_{elec}}\left(\frac{\omega}{\omega_1^*}\right)^4}{\sqrt{\left(1-\left(\frac{\omega}{\omega_1^*}\right)^2\right)^2\left(\alpha-\left(\frac{\omega}{\omega_1^*}\right)^2\right)^2}} \quad (14)$$

This maximum power becomes infinite at resonance, because the damping was initially neglected. Fig. 8 gives a plot of this matched power.

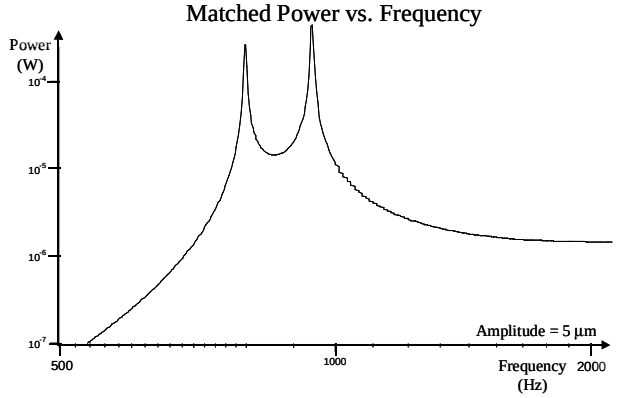

Figure 8: Resonance shift due to load matching.

Two symmetric capacitors

Two symmetric capacitors attached to the same mass, as is the case for the device in Fig.1, are modeled following the same method as for a single-sided capacitor. This results in Fig. 9 and Fig 10, which show the large-signal, respectively the small-signal models. The output power is given by equation (15):

$$P_{double-sided}(\omega)=\frac{\left(\frac{\omega}{\omega_1^*}\right)^4\left(\frac{\omega}{\omega_2}\right)^2\frac{4\Gamma^2}{C_0^2}\frac{Y^2}{4R}}{\left(1-\kappa^2-\left(\frac{\omega}{\omega_1^*}\right)^2-2\zeta*\frac{\omega^2}{\omega_2\omega_1*}\right)^2+\left(\frac{\omega}{\omega_2}\right)^2\left(1-\left(\frac{\omega}{\omega_1^*}\right)^2+2\zeta*\frac{\omega_2}{\omega_1*}\right)^2} \quad (15)$$

This equation indicates that two symmetric capacitors show the same behavior as the single capacitor described above, with the following considerations:

- as the system is symmetric, the charge flows from C_1 to C_2, and no current flows from electrode (B) to node (A). The formula for the single-sided case remains valid if Celec is set to infinite. The cut-off frequency ω_2 is now given by:

$$\omega_2=1/RC_0 \quad (16)$$

- as there are two resistors in series, the load resistor R has to be replaced by 2R.
- as there are two capacitors in series, the capacitor C_0 has to be replaced by $C_0/2$.

If C_{elec} is set to infinite, the value α becomes $1-\kappa^2$. The resonance frequency for low load resistances is then equal to the mechanical resonance frequency ω_1.The behavior of the device is thus analogous to the result of the analysis above.

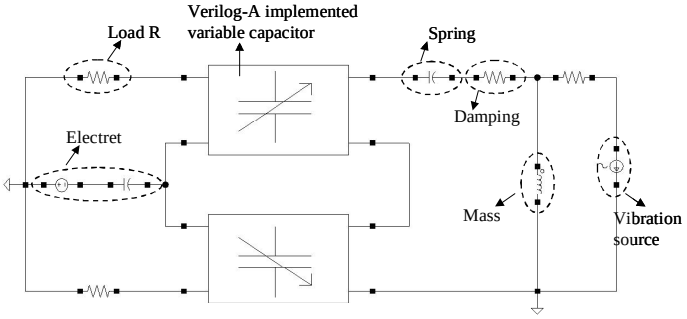

Figure 9: Large signal model of the device in Fig. 1 implemented in SPICE.

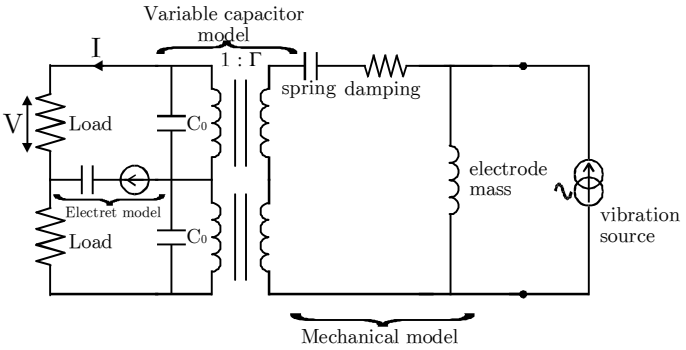

Figure 10: Linearized circuit of the device in Fig. 1.

DISCUSSION

The optimal design of an electrostatic generator strongly depends on the application it is designed for. The vibrations available in its intended environment should be analyzed, and a power peak frequency should be selected. The process flow is similar to standard accelerometer flows.

In order to get a hard feedback on the modeling, a prototyping process flow has been developed which makes use of commercially available SOI-technology, intended for accelerometer design. Although the design restrictions related to this process flow prevent the optimal design towards realistic low frequencies, the working principles will be verified and feedback will be available towards a custom made process flow.

The electret consists of a SiO_2-Si_3N_4 double-layer. The electret is charged by the corona around a pointed electrode when a high potential is applied between the tip and the substrate (Fig. 11). The air in the corona is ionized by the high field and the ions accelerate towards the surface of the electret. Charges are trapped in surface-traps and in traps at the oxide-nitride-interface [22]. The control grid determines the initial surface potential. To prevent fast discharge, the sample is made hydrophobic with an HMDS-treatment (hexamethyldisilazane). This way the lifetime of an electret reaches a few decades [23].

The bonding of both wafers has to be a low temperature process to preserve the electret. At the same time the gap between the wafers has to be small (C_{elec} large), but large enough to minimize damping.

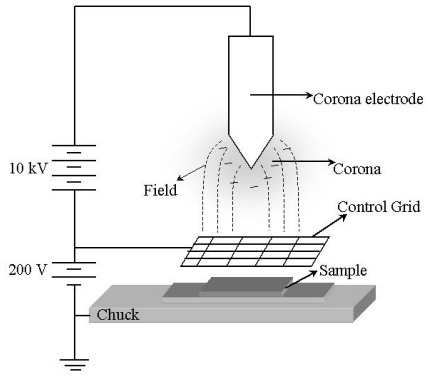

Figure 11: Corona charging set-up.

REALISATION

The first prototype process flow is designed to obtain a quick feedback on the modeling. The comb-resonator structure is therefore realized by a process designed for accelerometers, available in MPW. This structure is fabricated with an Epi-SOI surface micromachining technology [24]. We propose the following process flow to realize the electret and combine both elements to an electret-based generator.

On a highly doped silicon wafer (Fig. 12) a 400 nm thick thermal oxide was grown (wet) at 1050°C. On the oxide a 150 nm thick LPCVD silicon-nitride layer was deposited (12a). Those two layers form the electret (12b). To form a backside contact an Al-layer is evaporated (12c). The electret is patterned (12d); a resist rim is defined by lithography (12e). This resist defines the gap between the electret and the variable capacitor after both parts are combined.

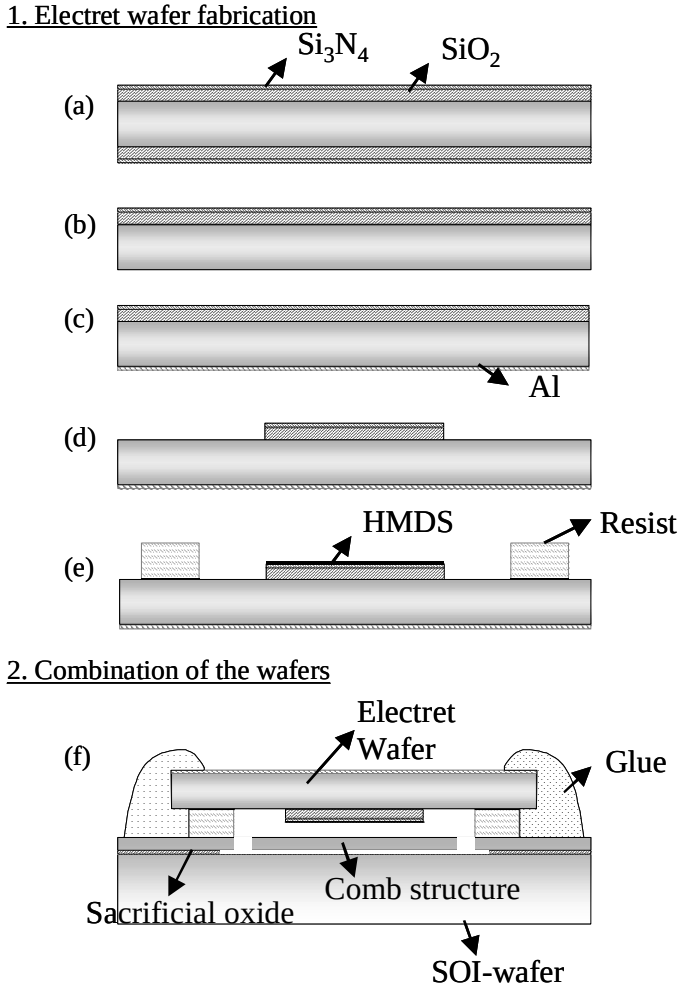

Figure 12: Process flow used to make and combine the electret and the MPW-wafer.

The electret is treated with HMDS to make the electret hydrophobic. The electret is then diced and aligned by flip-chip to the MPW-variable capacitor (12f). To obtain a rigid mechanical joint, glue is dispensed over the edges of the electret die.

RESULTS

This prototype variable capacitor has a total length of 2.4 mm and a width of 1.1 mm, occupying a surface of about 2.65 mm^2 (Fig 13). In this area two times 255 comb-pairs are realized to obtain two capacitance of 0.6 pF. The maximum displacement is fixed to 25 μm by stoppers, to obtain an 83% capacitance swing. The resonance frequency is 1140 kHz. The thickness of the mass is restricted to 20 μm because of the SOI-process flow. The gap between the fingers is 2.2 μm.

The beams that act as springs have a meandering structure to reduce the spring constant. Simulations indicated that the spring stiffening effect is reduced by the presence of the meanders.

These data, combined with an electret voltage of 150V, are simulated to generate 1 μW at 1020 Hz and 16 μW at 3750 Hz for a vibration with an amplitude of 20 μm. This output power is lower than the output of the simulated illustrator device due to the limitations on the mass and damping, as these are defined by the SOI-process.

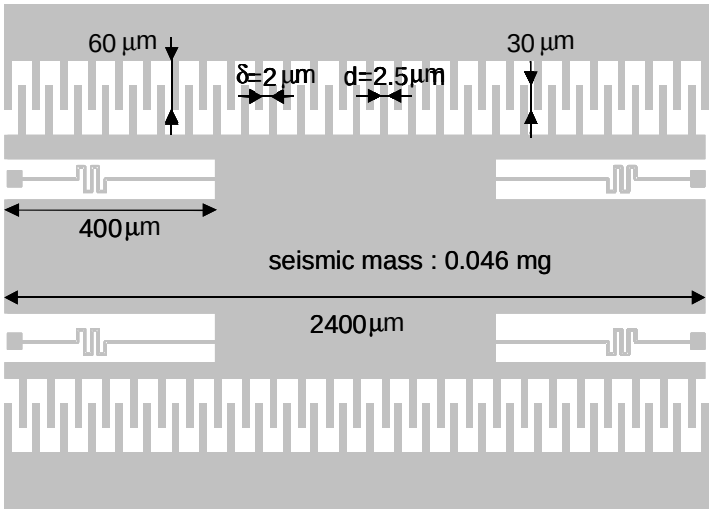

Figure 13: Layout overview of demonstrator device.

CONCLUSION

A new approach to electrostatic energy conversion has been proposed and modeled. The large signal model allows simulation of any generator-based circuit in any ambient mechanical conditions. A small signal model was used for evaluating the influences of the design parameters on the output characteristics, leading towards the design of a variable capacitor, based on a SOI-process available in MPW-service. According to this feasibility study, 40 µW electrical power is available at 930 Hz for a device displacement of only 5 mm^2.

ACKNOWLEDGEMENTS

We would like to thank Dr. Paolo Fiorini, Bert Dubois and Agnes Verbist for the discussions and the useful comments. Also we would like to thank Omar A.A. Nasr for the help on the modeling.

REFERENCES

[1] "Vibration-to-electric energy conversion", *Meninger, S.; Mur-Miranda, T.O.; Amirtharajah, R.; Chandrakasan, A.; Lang, J.*, International Symposium on Low Power Electronics and Design, pp. 48 –53 (1999)

[2] "Intelligent and low power sensor interface systems for biotelemetry applications", *Wouter, P.*; PhD Thesis, K.U.Leuven (1995)

[3] "Implantable Biotelemetry Devices for Animal Monitoring and Identification", *Wouters, P.; Puers, R.; Geers, R.; Goedseels, V.*, Engineering in Medicine and Biology Society, **Vol. 14**, Proceedings of the Annual International Conference of the IEEE, **Vol. 6,** pp. 2665 –2666 (1992)

[4] "IEE 802.15.4 : A developing Standard for Low-Power Low-Cost Wireless Personal Area Networks", *Gutierrez, J.A.; Naeve, M.; Callaway, E; Bourgeois, M.; Mitter, V.; Heile, B.;* IEEE network (2001)

[5] BioTronik, Technical Manual Philos

[6] "Microsystems and energy: the role of energy", *Goemans P.A.F.M.;* Microsystems technology: exploring opportunities, STT (1994)

[7] "Feasibility of micro power supplies for MEMS", *Koeneman P.B.; Busch-Vishniac I.J.; Wood K.L.;* Journal of microelectromechanical systems, **Vol. 6**, No. 4 (1997)

[8] "A six-wafer combustion system for a silicon micro gas turbine engine", *Mehra, A; Xin Zhang; Ayon, A.A.; Waitz, I.A.; Schmidt, M.A.; Spadaccini, C.M.;* Journal of Micro-electromechanical Systems, Vol. 9, No. 4, pp. 517-527 (2000)

[9] "A Microturbine Made by Micro-Electro-Discharge Machining", Peirs, J.; Reynaerts, D.; Verplaetsen, F.; Poesen, M.; Renier, PJ.; Eurosensors XVI, pp. 790-793, (2002)

[10] http://www.ndim.edrc.cmu.edu/papers/partnership.pdf

[11] "Development of a Transcutaneous Energy and Data Transmission System for High Power Applications up to 20 Watts", *Vandevoorde, G.; Catrysse, M.; Puers, R.; Beale, G.; Smith, P.; Sangster, A.;* Int. Symposium on Biotelemetry, pp. 580 (2000)

[12] "A Laser-micromachined Vibrational to Electrical Power Transducer for Wireless Sensing Systems", *Ching, N.N.H., Wong, H.Y., Li, W.J., Leong, P.H.W., Wen, Z.*; 11th Int. Conf. on Solid-State Sensors and Actuators *(Transducers '01)* (2001)

[13] "Towards a Piezoelectric Vibration-powered microgenerator", *Glynne-Jones, P.; Beeby, S.P.; White, N.M.;* IEE Proceedings on Science, Measurement and Technology, **Vol. 148,** No. 2, pp. 68-72 (2001)

[14] "Vibration-to-Electric Energy Conversion", *Meninger, S.; Mur-Mirande, J.O.; Amirtharajah, R.; Chandrakasan, A.P.; Lang, J.H;* Transcations on VLSI systems, **Vol. 9**, No. 1 (2001)

[15] "Capacitance Based Microstructures for Converting Vibrational Energy to Electric Energy", *Roundy, S.; D'Souza, R.;* madmax.me.berkeley.edu/~shadr/ MEMSFinProj.pdf

[16] "A Micromachined Capacitive electret microphone", *Thielemann, C.; Hess, G.*; SPIE, **Vol. 3680,** pp. 748-756 (1999)

[17] "A Micromachined Thin Film Teflon Electret Microphone", *Hsieh, W.H.;Hsu, T.Y.;Tai, Y.C.;*

[18] "Electrets", *Sessler, G.M.*; Topics in Applied Physics, **Vol. 33**, Springer-Verlag (1980)

[19] "On the Charge Storage and Decay Mechanism in Silicon Dioxide", *Olthuis, W.; Bergveld, P.;*IEEE Transactions on Electrical Insulation, **Vol. 27**, No. 4, pp. 691-697, (1992)

[20] "Inleiding mechanica en transductietechniek", *Elwenspoek, M.; Krijnen, G.;* course notes Utwente (1999)

[21] "Equivalent Circuit Representation of Electromechanical Transducers: I, Lumped-parameter systems", *H.A.C. Tilmans*, J. Micromech. Microeng. **Vol. 6**, pp. 157-176 (1996)

[22] "Inorganic Electret Layers For Miniaturized Devices"; *Amjadi, H.; Sessler, G. M.;* Conf. on Electrical Insulation and Dielectric Phenomena, pp. 668-671 (1995)

[23] "Electrets"; *Sessler, G.M.;* Topics in Applied Physics, **Vol. 33**, Springer-Verlag (1980)

[24] http://www.tronics-mst.com/memsoi.html